

# B Meson Decay Constants From NRQCD

A.Ali Khan<sup>a</sup>, T.Bhattacharya<sup>b</sup>, S.Collins<sup>c</sup>, C.T.H.Davies<sup>c</sup>, R.Gupta<sup>b</sup>,  
C.Morningstar<sup>d</sup>, J.Shigemitsu<sup>a</sup>, J.Sloan<sup>e</sup>.

<sup>a</sup>Physics Department, The Ohio State University,  
Columbus, OH 43210, USA.

<sup>b</sup>T-8, Los Alamos National Laboratory,  
Los Alamos, NM 87545, USA.

<sup>c</sup>Department of Physics & Astronomy, University of Glasgow,  
Glasgow, UK G12 8QQ.

<sup>d</sup>Physics Department, University of California at San Diego,  
La Jolla, CA 92093, USA.

<sup>e</sup>Physics Department, University of Kentucky,  
Lexington, KY 40506, USA.

May 1998

## Abstract

We present quenched results for  $B$  meson decay constants using NRQCD  $b$  quarks and  $O(a)$  tadpole improved clover light quarks. For the first time, one-loop matching factors between lattice and continuum currents are incorporated through  $O(\alpha/M)$  taking operator mixing fully into account. This includes an important  $O(\alpha a)$  discretization correction to the heavy-light axial vector current. We find  $f_B = 147(11)(^{+8}_{-12})(9)(6)\text{MeV}$  and  $f_{B_s}/f_B = 1.20(4)(^{+4}_{-0})$ .

PACS numbers: 12.38.Gc, 12.39.Hg, 13.20.He, 14.40.Ndi

## 1 Introduction

The  $B$  meson decay constant  $f_B$  and the bag parameter  $B_B$  play crucial roles in analyses of  $B_0 - \bar{B}_0$  mixing phenomena and the extraction of CKM matrix elements. Experimental

determination of  $f_B$  is severely constrained by the very small leptonic branching fraction, while  $B_B$  is not a direct outcome of experiments. Their calculation has proven difficult due to the possibility of large QCD corrections to the basic weak process. Lattice QCD provides a non-perturbative method for calculating the relevant hadronic matrix elements from first principles [1]. This paper presents a quenched lattice calculation of  $f_B$  and  $f_{B_s}$  using the non-relativistic QCD (NRQCD) approach to  $b$ -quarks [2]. Much of our discussion of the systematic improvement of  $f_B$ , however, applies to other lattice calculations of this quantity.

In the rest frame of the  $B$  meson, the momentum of the  $b$ -quark is of  $O(\Lambda_{QCD})$ . The  $b$ -quark velocity is hence  $v \approx \Lambda_{QCD}/M \approx 0.1$ , where  $M$  is the heavy quark mass, and the non-relativistic approach is sensible. The heavy quark action that we employ includes relativistic corrections through  $O((\Lambda_{QCD}/M)^2)$ . For the light quarks we use the tree-level tadpole improved clover action which reduces  $O(a\Lambda_{QCD})$  errors to  $O(\alpha(a\Lambda_{QCD}))$  [3]. In the heavy-light axial current we investigate both  $1/M$  and  $1/M^2$  corrections. The one-loop matching factors relating the lattice and full (relativistic) continuum QCD currents have been calculated to  $O(\alpha/M)$  [4] and incorporated in this analysis. Mixing among heavy-light current operators and contributions from an  $O(\alpha(a\Lambda_{QCD}))$  discretization correction to the current are taken into account. In the nonrelativistic approach the  $1/M$  expansion and  $O(a)$  improvements go hand in hand. Previous calculations of  $f_B$  using NRQCD  $b$ -quarks have included only subsets of the above ingredients [5, 6, 7], as have calculations using the relativistic formalism for the  $b$ -quark [8, 9, 10, 11, 12]. Here we include all of them and carry out a comprehensive study with improvements through  $O((\Lambda_{QCD}/M)^2)$  and  $O(a\Lambda_{QCD})$  in the action and through  $O((\Lambda_{QCD}/M)^2)$ ,  $O(\alpha/(aM))$ ,  $O(\alpha(\Lambda_{QCD}/M))$  and  $O(\alpha(a\Lambda_{QCD}))$  in the currents.

## 2 Details of the Simulation

The NRQCD heavy quark action density used in our lattice simulations is a variant of the one proposed in [2],

$$\mathcal{L} = \bar{\psi}_t \psi_t - \bar{\psi}_t \left(1 - \frac{a\delta H}{2}\right)_t \left(1 - \frac{aH_0}{2n}\right)_t U_4^\dagger \left(1 - \frac{aH_0}{2n}\right)_{t-1} \left(1 - \frac{a\delta H}{2}\right)_{t-1} \psi_{t-1}, \quad (1)$$

where  $\psi$  denotes a two-component Pauli spinor,  $H_0$  is the nonrelativistic kinetic energy operator,

$$H_0 = -\frac{\Delta^{(2)}}{2M_0}, \quad (2)$$

and  $\delta H$  includes relativistic and finite-lattice-spacing corrections,

$$\begin{aligned} \delta H = & -\frac{g}{2M_0} \boldsymbol{\sigma} \cdot \mathbf{B} \\ & + \frac{ig}{8(M_0)^2} (\nabla \cdot \mathbf{E} - \mathbf{E} \cdot \nabla) - \frac{g}{8(M_0)^2} \boldsymbol{\sigma} \cdot (\nabla \times \mathbf{E} - \mathbf{E} \times \nabla) \\ & - \frac{(\Delta^{(2)})^2}{8(M_0)^3} + \frac{a^2 \Delta^{(4)}}{24M_0} - \frac{a(\Delta^{(2)})^2}{16n(M_0)^2}. \end{aligned} \quad (3)$$

In addition to all  $1/M^2$  terms we have also included the leading  $1/M^3$  relativistic correction as well as the discretization corrections appearing at the same order in the momentum expansion.  $\nabla$  and  $\Delta^{(2)}$  are the symmetric gauge-covariant lattice derivative and laplacian, while  $\Delta^{(4)}$  is a discretized version of the continuum operator  $\sum D_i^4$ . The parameter  $n$  is introduced to remove instabilities in the heavy quark propagator due to the highest momentum modes [2]. For the heavy quark action, we use two-leaf  $\mathbf{E}$  fields [13] rather than the four-leaf fields of previous NRQCD simulations. The tree-level coefficients are tadpole-improved by rescaling the gauge fields by the fourth root of the plaquette,  $u_0 = 0.87779$  at  $\beta = 6.0$  [14]. For the light quarks we use the tree-level tadpole improved clover action ( $c_{SW} = u_0^{-3}$ ).

Simulations were carried out on 102 quenched configurations on  $16^3 \times 48$  lattices at  $\beta = 6.0$ . Both forward and time reversed quark propagators were calculated on each configuration in order to improve statistics. Error estimates are obtained using a bootstrap procedure. Meson correlators are calculated for 30 combinations of quark masses; five values for  $\kappa$  and six values for the bare heavy quark mass. Two of the  $\kappa$  values are selected to simulate the charm quark, and the remaining three are around the strange quark mass. Heavy quark masses range from below the bottom quark mass to about five times the bottom quark mass. Both the heavy and the light quark propagators were smeared at the sink and/or the source. Further details are given in Ref. [6].

There are four input parameters in the simulations, the light quark mass ( $\kappa_l \equiv \kappa_{u,d}$ ), the strange quark mass ( $\kappa_s$ ), the scale  $a^{-1}$ , and the heavy quark mass ( $M_0$ ). These need to be fixed via experimental input.

To set the scale one can use a variety of quantities like  $M_\rho$ ,  $f_\pi$ , string tension ( $\sigma$ ), or quarkonium S-P splittings. In quenched calculations, however, different physical quantities can lead to different  $a^{-1}$ 's and one must make a choice. In principle one would like to choose an observable whose characteristic momenta are similar to those of the quantities being calculated and which has comparable quenching and discretization errors. The first choice would be to fix  $a^{-1}$  from the heavy-light spectrum itself but experimental and numerical errors will have to be reduced before this becomes practical. Based on the ‘‘brown muck’’ picture of HQET for heavy-light systems [15], however, we believe that the scales relevant for energy splittings in heavy-light spectroscopy and for the decay constant are determined by the light quark dynamics. For  $f_B$  and spectroscopy we shall therefore consider observables in the light quark and gluonic sector to set the scale. For clover fermions at  $\beta = 6.0$ , the values for  $a^{-1}$  from  $M_\rho$ ,  $M_K$ ,  $M_N$ ,  $M_\Delta$ ,  $\sigma$ , and  $f_\pi$  range between 1.8 GeV and 2.0 GeV. We use  $a_{m_\rho}^{-1} = 1.92(7)$  GeV as it is close to the mean, and can be extracted most reliably from our data. We also calculate the final values using  $a^{-1} = 1.8$  and 2.0 GeV and use the spread as the uncertainty due to the determination of the scale.

We determine  $\kappa_l = 0.13917(9)$  by linearly extrapolating the pion mass, calculated on the same set of configurations, to the physical value. To set  $\kappa_s$  we use the  $K$ , the  $K^*$  and the  $\phi$ , which yields the values 0.13755(13), 0.13719(25), and 0.13717(25), respectively. We quote central values for our  $B_s$  meson decay constant using the  $K$ , and the difference between the  $K$  and  $\phi$  as a systematic error.

The bare heavy quark mass is fixed by linearly interpolating between the meson masses with the three lightest  $M_0$  values to the experimental  $B$  meson mass. Since the NRQCD action

$aM_0$	$\kappa_l$				$\kappa_s$			
	$aE_{sim}$	$aM_{kin}$	$aM_{pert}$	$aM'$	$aE_{sim}$	$aM_{kin}$	$aM_{pert}$	$aM'$
1.6	0.422(6)	2.17(24)	2.08(09)	2.11(5)	0.483(8)	2.21(13)	2.14(09)	2.17(5)
2.0	0.438(7)	2.57(33)	2.46(10)	2.52(6)	0.499(8)	2.63(18)	2.52(10)	2.58(6)
2.7	0.452(8)	3.34(58)	3.12(11)	3.26(8)	0.513(8)	3.37(29)	3.18(11)	3.32(8)
4.0	0.461(9)	5.2(1.5)	4.32(10)	4.59(9)	0.522(8)	4.86(67)	4.38(10)	4.65(9)

Table 1: Simulation energies and pseudoscalar meson masses in lattice units for light and strange clover quark masses. Meson masses are determined from eq.(4) with  $\Delta$  coming from perturbation theory ( $M_{pert}$ ) or heavy-heavy spectroscopy ( $M'$ ), and from the dispersion relation eq.(5) ( $M_{kin}$ ).

omits the heavy quark rest mass, heavy-light pseudoscalar meson masses are not direct outputs of the simulations. Instead, correlation functions fall off with an energy  $E_{sim}$  that is related to the full meson mass  $M_{PS}$  and the bare  $b$ -quark mass  $M_0$  as,

$$M_{PS} = \Delta + E_{sim} \equiv [Z_m M_0 - E_0] + E_{sim}, \quad (4)$$

where  $Z_m$  is the mass renormalization constant and  $E_0$  an energy shift.  $Z_m$  and  $E_0$  have been calculated perturbatively and  $E_{sim}$  is obtained nonperturbatively from the simulations. An alternate way to obtain the meson mass is to calculate energy splittings between correlators with and without spatial momentum,

$$E_{sim}(\vec{p}) - E_{sim}(0) = \sqrt{\vec{p}^2 + M_{kin}^2} - M_{kin}. \quad (5)$$

In Table 1 we list results for  $M_{PS}$  of eq.(4) using perturbation theory to calculate  $\Delta$  (denoted “ $M_{pert}$ ” in the Table) and for  $M_{kin}$  of eq.(5), both measured in units of  $a^{-1}$ .  $\Delta$  can also be obtained nonperturbatively from simulations of quarkonium  $\bar{Q}Q$  systems, whose correlations fall off with an energy  $E_{sim}^{\bar{Q}Q}$  related to the full  $\bar{Q}Q$  meson mass as,

$$M_{\bar{Q}Q} = M_{kin}^{\bar{Q}Q} = 2 \Delta + E_{sim}^{\bar{Q}Q}. \quad (6)$$

Both  $M_{kin}^{\bar{Q}Q}$  and  $E_{sim}^{\bar{Q}Q}$  can be extracted from the simulations, leading to a nonperturbative determination of  $\Delta$ . The resulting masses for the heavy-light mesons are also listed in Table 1 under  $aM'$ . One finds consistency among the three determinations of the meson mass,  $aM_{kin}$ ,  $aM_{pert}$  and  $aM'$ , in most cases, to within  $1\sigma$ . The errors for  $aM_{kin}$  are much larger than for  $aM'$  since finite momentum correlators have much larger fluctuations for heavy-light mesons than for heavy-heavy mesons. The errors on  $aM_{pert}$  were estimated by squaring the one-loop corrections and by varying  $q^*$ , the scale in the coupling  $\alpha$ . We will use the most accurately determined  $aM'$  to fix  $aM_0$ . With  $a^{-1} = 1.92(7)$  GeV and using linear interpolation between the three lightest heavy quark masses, one finds that  $aM_0 = 2.22(11)$  gives the correct  $B$  meson mass. Had one used  $aM_{kin}$  rather than  $aM'$ , the number changes to  $aM_0 = 2.28(42)$ . The effect of this difference on  $f_B$  is invisible.

The results for the heavy-light spectrum, including radially excited states, P-states and heavy baryons, based on the same data set, are summarized in Figure 1. We find that the

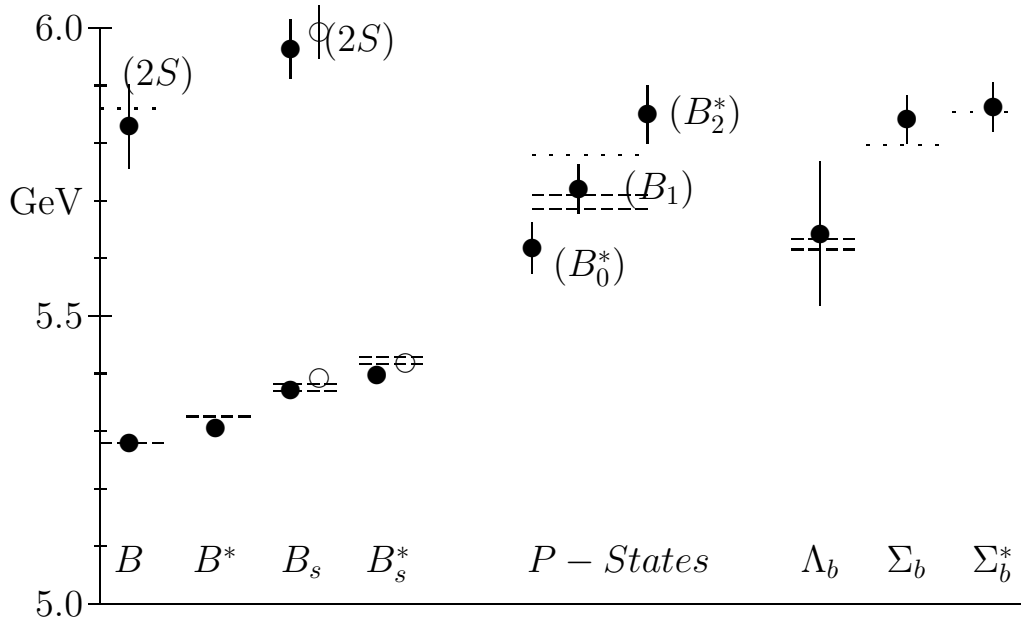


Figure 1: Heavy-light spectrum with  $b$ -quarks. Horizontal dashed lines bracket experimental values taken from the Particle Data Book. Horizontal dotted lines indicate first experimental observations of these states ([17] ( $2S$  &  $1^{+'}/B_2^*$ ) and [18] ( $\Sigma_b$ )). Errors on simulation results include statistical plus, where appropriate, errors from extrapolation in the light quark mass to the physical pion. The two results for the strange  $B$  mesons correspond to fixing the strange quark mass from either the  $K$  (filled circles) or the  $\phi$  (open circles). For the  $J = 1$  P states only one level is shown, since we are currently unable to reliably separate the physical  $1^+$  and  $1^{+'}$  states.

combination, NRQCD heavy and clover light quarks, reproduces the gross features of the  $B$  mesons and the heavy baryons. This is a prerequisite for a reliable calculation of  $f_B$ . Details of the spectrum calculations will be given in a separate publication [16].

### 3 Heavy-Light Axial Currents in NRQCD and Matching to Continuum Full QCD

The goal is to calculate the pseudoscalar decay constant  $f_{PS}$ , defined in Euclidean space through the relation,

$$\langle 0 | A_\mu | PS \rangle = p_\mu f_{PS}. \quad (7)$$

Here  $A_\mu$  is the heavy-light axial vector current in full continuum QCD. One needs to relate this current to the current operators  $J_L^{(i)}$  in lattice NRQCD.

Heavy-light currents in full continuum QCD have the form  $\bar{q}\Gamma h$ . For  $A_0$ , we use  $\Gamma = \gamma_5\gamma_0$ . The four-component Dirac spinor for the heavy quark,  $h$ , is related to the two-component NRQCD heavy quark (heavy anti-quark) fields,  $\psi$  ( $\tilde{\psi}$ ), via an inverse Foldy-Wouthuysen transformation:

$$h = U_{FW}^{-1} \Psi_{FW} = U_{FW}^{-1} \begin{pmatrix} \psi \\ \tilde{\psi} \end{pmatrix}. \quad (8)$$

Through  $O(1/M^2)$  this gives,

$$\begin{aligned} \bar{q}\Gamma h &= \bar{q}\Gamma Q - \frac{1}{2M} \bar{q}\Gamma(\boldsymbol{\gamma} \cdot \mathbf{D})Q \\ &+ \frac{1}{8M^2} \bar{q}\Gamma \left( \mathbf{D}^2 + g\boldsymbol{\Sigma} \cdot \mathbf{B} - 2ig\boldsymbol{\alpha} \cdot \mathbf{E} \right) Q, \end{aligned} \quad (9)$$

where  $Q = \frac{1}{2}(1 + \gamma_0)\Psi_{FW}$  and  $\boldsymbol{\alpha} \equiv \gamma_0\boldsymbol{\gamma}$ ,  $\boldsymbol{\Sigma} = \text{diag}(\boldsymbol{\sigma}, \boldsymbol{\sigma})$ . In our simulations we have included all tree-level contributions to the current through  $O(1/M^2)$  using the terms in eq.(9).

We use perturbation theory to match between the lattice currents in our simulations and those of continuum QCD and employ on-shell matching conditions. One starts by considering the process in which a heavy quark of momentum  $p$  is scattered by the heavy-light current into a light quark of momentum  $p'$ . Matching takes place by requiring that the amplitude for this process calculated in full QCD agrees with that in the effective theory through the order in  $\alpha$  and  $1/M$  that one is working in. Here we work through  $O(\alpha/M)$ . The amplitude in full QCD can be expanded in terms of  $p/M$ ,  $p'/M$  etc. The next step is to identify current operators in the effective theory that would reproduce the same terms in the amplitude. Finally, a one-loop mixing matrix calculation must be done within the effective theory. Details of such a matching calculation are given in [4]. Here we summarize the main features.

The full QCD calculation uses naive dimensional regularization (NDR) in the  $\overline{MS}$  scheme. A gluon mass  $\lambda$  is introduced at intermediate stages of the calculation to regulate IR divergences. This is permissible here since no non-Abelian vertices appear in this one-loop calculation. A one-loop calculation in full QCD finds, upon expanding through  $O(1/M)$ , that the following three current operators are required in the lattice effective theory:

$$\begin{aligned} J_L^{(0)} &= \bar{q}\gamma_5\gamma_0 Q, \\ J_L^{(1)} &= -\frac{1}{2M} \bar{q}\gamma_5\gamma_0(\boldsymbol{\gamma} \cdot \nabla)Q, \\ J_L^{(2)} &= \frac{1}{2M} \bar{q}(\boldsymbol{\gamma} \cdot \overleftarrow{\nabla})\gamma_5\gamma_0 Q. \end{aligned} \quad (10)$$

$J_L^{(0)}$  and  $J_L^{(1)}$  correspond to discretized versions of the first two terms in eq.(9),  $J_L^{(2)}$  appears only at one loop. After carrying out a one-loop mixing matrix calculation in lattice NRQCD, one ends up with the final matching relation between  $\langle A_0 \rangle$  in full QCD and matrix elements evaluated in the lattice simulations,

$$\langle A_0 \rangle_{QCD} = \sum_j C_j \langle J_L^{(j)} \rangle. \quad (11)$$

$C_0$ ,  $C_1$  and  $C_2$  are the three matching coefficients. Relation (11) is independent of the external states up to lattice artefacts.

An interesting outcome of the one-loop calculation is that the mixing between  $J_L^{(0)}$  and  $J_L^{(2)}$  does not vanish in the limit  $M \rightarrow \infty$ . This is because of the generation of a term, at order( $a\alpha$ ), which is a lattice artefact. This term can be absorbed into an  $O(\alpha(a\Lambda_{QCD}))$  discretization correction to  $J_L^{(0)}$ :

$$J_L^{(0)} \rightarrow J_L^{(0)} + C_A J_L^{(disc)}, \quad (12)$$

with

$$J_L^{(disc)} = a \bar{q} (\boldsymbol{\gamma} \cdot \overleftarrow{\nabla}) \gamma_5 \gamma_0 Q. \quad (13)$$

The coefficient  $C_A$  is also calculated in [4].  $J_L^{(disc)}$  is the analogue in heavy-light physics of the  $a \partial_\mu P$  discretization correction to the light quark axial current (here  $P$  is the pseudoscalar density) of Ref. [19].

The matching coefficients  $C_j$  are functions of the coupling  $\alpha$  and of the heavy quark mass and one needs to specify the precise definitions of these parameters. We use  $\alpha_V(q^*)$  of reference [14] as our perturbative expansion parameter. The scale  $q^*$  is not yet known for this matching calculation, however, a value for the  $M \rightarrow \infty$  limit has been calculated in reference [20] and gives  $q^* = 2.18/a$ . We shall extract  $f_B$  for  $q^* = 1/a$  and  $q^* = \pi/a$  and use the difference between the two as an estimate of the  $\alpha^2$  uncertainty. It is also important to use a common definition for the heavy quark mass in the continuum and lattice calculations. This can be ensured in perturbation theory by employing on-shell quark mass renormalization and using the pole mass in both theories. After writing everything in terms of the pole mass, we convert to the bare lattice mass  $M_0$ , which is a well defined quantity even beyond perturbation theory and the mass that appears in our lattice simulations. We use one-loop perturbation theory for this conversion.

Once  $O(1/M^2)$  corrections to the current are included at tree level, eq.(11) is modified to,

$$\langle A_0 \rangle_{QCD} = \sum_{j=0,1,2} C_j \langle J_L^{(j)} \rangle + \sum_{j=3,4,5} \langle J_L^{(j)} \rangle, \quad (14)$$

with  $J_L^{(j)}$ ,  $j = 3, 4, 5$ , corresponding to the three  $1/M^2$  current corrections in eq.(9). The matching coefficients  $C_j$ ,  $j = 0, 1, 2$ , do not include one-loop feedback from these latter  $1/M^2$  current operators. Such contributions come in at  $O(\alpha/M^2)$ . Eq.(14) is the NRQCD/Clover heavy-light axial current we use to extract  $f_{PS}$ . It includes terms through  $O((\Lambda_{QCD}/M)^2)$ ,  $O(\alpha \Lambda_{QCD}/M)$ ,  $O(\alpha/(aM))$  and  $O(\alpha(a\Lambda_{QCD}))$ . We note that powers of both  $1/(aM)$  and  $\Lambda_{QCD}/M$  are contained in our expressions. These ratios are both considered small in the NRQCD formalism (in practice  $1/(aM)$  is sometimes allowed to become as large as  $\sim 1$ ). In particular, one does not take the limit  $aM \rightarrow 0$ . The cutoff and therefore momenta allowed cannot become larger than  $\sim M$  in a non-relativistic theory.

We end this section with two brief comments. The first concerns non-perturbative effects that arise because we have power-law contributions to the matching coefficients that go as  $\alpha/(aM)^n$ . These terms are not separated out explicitly in our calculations but they are evident if coefficients are plotted as a function of  $aM$ . They are there to cancel unphysical ultra-violet pieces in the NRQCD current matrix elements, which do not match full QCD. It is possible for the  $\alpha/(aM)^n$  terms in, say,  $C_0$  to multiply non-perturbative lattice errors,  $\propto (a\Lambda_{QCD})^n$ , in

the matrix element  $\langle J_L^{(0)} \rangle$  to give contributions that look like physical  $(\Lambda_{QCD}/M)^n$  corrections to  $f_B$ . This limits our ability to extract the physical  $M$  dependence of  $f_B$ . The source of these non-perturbative errors is a mis-match between the infra-red physics of lattice NRQCD and that of full QCD. After taking the improvement of eq.(12) into account our  $\langle J_L^{(0)} \rangle$  is designed to match full QCD through  $O(\alpha a)$ . So these errors appear at  $O(\alpha^2 (a\Lambda_{QCD}))$  or  $O((a\Lambda_{QCD})^2)$ . The leading contribution to  $f_B$  from these non-perturbative lattice artefacts is then  $\alpha/(aM) \times \alpha^2 (a\Lambda_{QCD}) = \alpha^3 \times \Lambda_{QCD}/M$  or  $\alpha/(aM) \times (a\Lambda_{QCD})^2 = \alpha (a\Lambda_{QCD}) \times \Lambda_{QCD}/M$  giving an error in the slope of  $O(\alpha^3)$  or  $O(\alpha (a\Lambda_{QCD}))$ . Both these terms are of the same order as higher order corrections not yet included in our matching calculations; they do not lead to any fundamental difficulties. Better precision can be attained in principle by going to more highly improved actions and current operators. Conversely we note that the situation is considerably worse for Wilson light quarks where discretization errors in the action mean that the currents cannot be improved to the level we have achieved here. Then non-perturbative lattice artefacts could induce an  $\alpha/(aM) \times (a\Lambda_{QCD}) = \alpha (\Lambda_{QCD}/M)$  error in  $f_B$ .

The second comment concerns cancellation of the power-law contributions referred to above. For instance, our matrix elements will contain unphysical contributions that behave as  $\alpha/(aM)$  and which are cancelled by the perturbative matching procedure. This might be a delicate operation if the terms behaving as  $\alpha/(aM)$  in the matching coefficients and in the matrix elements were much larger than the physical terms of  $O(\Lambda_{QCD}/M)$ . In the region in which we work none of the perturbative coefficients of the  $\alpha/(aM)$  terms are unduly large. No delicate cancellation is necessary. Furthermore the current matrix elements are clearly dominated by their physical components, in particular the matrix elements of the higher dimension operators,  $J_L^{(1)}$  and  $J_L^{(2)}$ , show no sign of significant  $\alpha/(aM)^n$  terms. This will be discussed in more detail elsewhere [21]. In our calculations power-law terms have been subtracted perturbatively through  $O(\alpha/(aM))$ . Uncancelled contributions would come in at  $O(\alpha^2/(aM))$  and  $O(\alpha/(aM)^2)$ . There is no indication from the behavior of our matrix elements that such contributions are particularly large. Any uncertainty arising from them will be covered by the systematic errors that we assign in the next section to higher order perturbative and relativistic corrections.

## 4 Results

Details of our data analysis for decay constants are described in [5, 6] and will not be repeated here. We start with the discussion of the size of the various terms in the lattice current defined in eq.(14). Table 2 summarizes our results for

$$f^{(j)} \sqrt{M_{PS}} = \frac{1}{\sqrt{M_{PS}}} \langle 0 | J_L^{(j)} | PS \rangle, \quad (j = 0 \dots 5), \quad (15)$$

evaluated at zero 3-momentum. The light quark has been extrapolated/interpolated linearly to  $\kappa_l$  or  $\kappa_s$ . The matrix elements of  $J_L^{(2)}$  are not shown as they are identical to  $J_L^{(1)}$  at zero 3-momentum. The data show that around the physical  $B$  ( $aM_0 = 2.22(11)$ ) the matrix elements of  $J_L^{(1)}$  are  $\sim 12\%$  of  $J_L^{(0)}$ . The analogous ratio for the sum of the three  $1/M^2$  currents (which



$aM_0$	$a^{3/2} f^{(0)} \sqrt{M}$	$a^{3/2} f^{(1)} \sqrt{M}$	$a^{3/2} f^{(3)} \sqrt{M}$	$a^{3/2} f^{(4)} \sqrt{M}$	$a^{3/2} f^{(5)} \sqrt{M}$
$\kappa_l$					
1.6	0.164(7)	-0.0245(12)	-0.0053(4)	0.00363(15)	-0.0050(3)
2.0	0.167(9)	-0.0206(10)	-0.0036(2)	0.00216(10)	-0.00325(19)
2.7	0.170(11)	-0.0162(10)	-0.00220(14)	0.00109(6)	-0.00181(13)
4.0	0.174(11)	-0.0113(8)	-0.00111(8)	0.00045(3)	-0.00082(5)
7.0	0.191(8)	-0.0075(4)	-0.00049(2)	0.000144(8)	-0.000287(15)
10.0	0.198(9)	-0.0055(2)	-0.000272(12)	0.000072(5)	-0.000145(8)
$\kappa_s$					
1.6	0.194(5)	-0.0278(8)	-0.00635(17)	0.00420(11)	-0.00576(17)
2.0	0.198(6)	-0.0236(7)	-0.00446(15)	0.00253(7)	-0.00375(12)
2.7	0.205(7)	-0.0187(6)	-0.00276(10)	0.00129(4)	-0.00210(8)
4.0	0.212(8)	-0.0134(5)	-0.00144(6)	0.00054(2)	-0.00098(3)
7.0	0.230(6)	-0.0088(2)	-0.000620(17)	0.000171(5)	-0.000341(10)
10.0	0.237(6)	-0.0065(17)	-0.000344(9)	0.000083(3)	-0.000171(5)

Table 2: Tree-level matrix elements, in lattice units.  $f^{(j)}$  is defined in eq.(15).

partially cancel) is  $\sim 3\%$ . It is therefore reasonable to assume that the neglected  $1/M^3$  and higher terms are  $\leq 1\%$ .

The results for  $a^{3/2} f_{PS} \sqrt{M_{PS}}$  with the one-loop matching coefficients are summarized in Table 3. We show results for three values of  $\alpha$ : 0,  $\alpha_V(q^* = 1/a)$  and  $\alpha_V(q^* = \pi/a)$ . Two of the matching coefficients,  $C_0$  and  $C_1$ , include a term  $\alpha \ln(aM)/\pi$ . In Table 3 we have used the dimensionless bare heavy quark mass,  $aM_0$ , for the argument of these logarithms. There are no problems with large logarithms around the physical  $B$  meson, however, if one were to work at large  $aM_0$ , resumming the logarithms would be more appropriate. At the  $B$  meson, the one-loop correction decreases the decay constant by  $\sim 9 - 14\%$  depending on  $q^*$  of which  $\sim 3 - 5\%$  are due to the one-loop contributions from  $J_L^{(1)}$ ,  $J_L^{(2)}$  and  $J_L^{(disc)}$ . The  $\sim 5\%$  uncertainty coming from the variation in  $q^*$  will be taken as a measure of the uncertainty coming from higher order perturbative corrections. This is a conservative assignment of  $\sim 50\%$  of the one-loop correction. The perturbative matching coefficients employed in this article used the full  $1/M^2$  action of eq.(1) with  $\delta H$  given by eq.(3) (with, however, four-leaf  $\mathbf{E}$  fields). Matching coefficients from an  $O(1/M)$  NRQCD action (with  $\delta H = -\frac{g}{2M_0} \boldsymbol{\sigma} \cdot \mathbf{B}$ ) are also available [4] and lead to a difference in  $f_B$  of about  $\sim 1\%$ . This comparison gives us some idea of the effect from  $O(\alpha/M^2)$  contributions to matching coefficients on  $f_B$ . We will assign a  $\sim 4\%$  error to the full  $O(\alpha/M^2)$  corrections from the  $1/M^2$  current operators. This is the size of  $\alpha/(aM_0)^2$  and is more conservative than using the tree level value of the  $1/M^2$  corrections. Adding this in quadrature to the  $\sim 5\%$   $O(\alpha^2)$  and  $\sim 1\%$   $O(1/M^3)$  errors gives a  $\sim 6\%$  systematic error from higher order perturbative and relativistic corrections. The dominant discretization errors in the present decay constant calculation are of  $O((a\Lambda_{QCD})^2)$ , giving an additional systematic error of  $\sim 4\%$ .

$aM_0$	$\kappa_l$			$\kappa_s$		
	tree-level	$q^* = \pi/a$	$q^* = 1/a$	tree-level	$q^* = \pi/a$	$q^* = 1/a$
1.6	0.133(7)	0.121(6)	0.114(6)	0.158(5)	0.144(4)	0.136(4)
2.0	0.142(8)	0.128(7)	0.121(7)	0.169(5)	0.153(5)	0.144(5)
2.7	0.151(10)	0.135(9)	0.127(9)	0.182(7)	0.164(6)	0.153(6)
4.0	0.162(10)	0.144(10)	0.135(9)	0.196(7)	0.176(6)	0.164(6)
7.0	0.183(8)	0.162(7)	0.150(7)	0.220(6)	0.195(5)	0.181(5)
10.0	0.193(9)	0.170(8)	0.158(8)	0.231(6)	0.204(6)	0.189(5)

Table 3: Decay matrix elements  $f\sqrt{M}$  in lattice units. The first column gives tree-level results, the second includes renormalization constants using  $\alpha_V$  at  $q^* = \pi/a$ , and the third using  $\alpha_V$  at  $q^* = 1/a$ .

$a^{-1}$ [GeV]	$aM_b^0$	$f_B$ [MeV]		$f_{B_s}$ [MeV]	
		$q^* = \pi/a$	$q^* = 1/a$	$q^* = \pi/a$	$q^* = 1/a$
1.8	2.39(7)	140(9)	131(8)	171(5)	160(5)
1.92	2.22(6)	151(9)	142(9)	180(6)	169(6)
2.0	2.11(6)	159(9)	150(9)	187(6)	176(6)

Table 4: Decay constants  $f_B$  and  $f_{B_s}$  in MeV. Statistical errors only are shown.  $aM_b^0$  is the dimensionless bare heavy quark mass which leads to the correct  $B$  meson mass.

Table 4 shows results for  $f_{PS}$  at the physical  $b$ -quark mass for several choices of the scale. For each scale,  $aM_b^0$  denotes the value of the dimensionless bare heavy quark mass which gives the correct  $B$  meson mass. Using the scale  $a_{m_p}^{-1} = 1.92(7)$  GeV and averaging over the two  $q^*$ 's, our final estimate in the quenched approximation is then,

$$\begin{aligned}
f_B &= 147(11)_{(-12)}^{(+8)}(9)(6)\text{MeV}, \\
f_{B_s} &= 175(08)_{(-10)}^{(+7)}(11)(7)_{(-0)}^{(+7)}\text{MeV}.
\end{aligned}
\tag{16}$$

The first error comes from statistics plus extrapolation/interpolations in  $\kappa$  and  $aM_0$ . Scale uncertainties are reflected in the second error with the upper and lower limits coming from  $a^{-1} = 2.0$  GeV or  $a^{-1} = 1.8$  GeV respectively. The third error is due to higher order relativistic and perturbative corrections and the fourth due to discretization corrections. The central value of  $f_{B_s}$  has been calculated fixing the strange quark mass from the  $K$  meson; the fifth error bar comes from the difference in  $\kappa_s$  from the  $\phi$  and the  $K$ .

Another quantity of interest is the ratio  $f_{B_s}/f_B$ . It can be determined to a greater accuracy than  $f_B$  and  $f_{B_s}$  separately, since the direct dependence on the lattice scale drops out, and the statistical errors partly cancel. We obtain this ratio for each value of the heavy mass using,

$$\frac{f_{B_s}}{f_B} = \frac{(f\sqrt{M})_{\kappa=\kappa_s}}{(f\sqrt{M})_{\kappa=\kappa_l}} \frac{\sqrt{M_B}}{\sqrt{M_{B_s}}},
\tag{17}$$

$aM_0$	tree-level	$q^* = \pi/a$	$q^* = 1/a$
1.6	1.18(4)(5)	1.18(4)(5)	1.19(4)(4)
2.0	1.19(4)(4)	1.19(4)(4)	1.19(4)(5)
2.7	1.20(5)(5)	1.20(5)(5)	1.21(5)(5)
4.0	1.21(5)(5)	1.21(5)(5)	1.21(5)(5)
7.0	1.19(4)(5)	1.20(4)(4)	1.20(4)(4)
10.0	1.19(4)(4)	1.19(4)(5)	1.19(4)(5)

Table 5:  $f_{B_s}/f_B$ , without renormalization constants (left),  $q^* = \pi/a$  (middle), and  $q^* = 1/a$ .

where  $M_B$  and  $M_{B_s}$  are the experimental meson masses. Table 5 shows our results. One sees that one-loop renormalization has negligible effect on  $f_{B_s}/f_B$ . This also indicates that the errors from higher orders in perturbation theory are negligible. In the range studied, the data do not show any significant dependence on  $aM_0$ . Linearly interpolating to  $aM_b^0$ , our best estimate of the ratio is

$$\frac{f_{B_s}}{f_B} = 1.20(4)_{(-0)}^{(+4)}. \quad (18)$$

The first error is statistical and the second error comes from the uncertainties in fixing  $\kappa_s$ .

Eqs. (16) and (18) give the main results of this article and represent the most complete results to date for  $f_B$  and  $f_{B_s}/f_B$  using NRQCD  $b$ -quarks. It is interesting to compare them with other calculations that have used a relativistic formalism for the heavy  $b$ -quark. Table 6 gives such a comparison with the APE [8], Fermilab [9], JLQCD [10], MILC [11] and UKQCD [12] collaborations. Details of the simulation parameters and analyses are different among these groups (for recent reviews see [1]). For example MILC uses the Wilson quark action, UKQCD and APE results are for the clover action with  $c_{SW} = 1$ , Fermilab uses tree-level tadpole improved clover and JLQCD uses one-loop tadpole modified clover. Only JLQCD, MILC and Fermilab extrapolate to  $a = 0$ , and JLQCD and Fermilab include  $M$ -dependent renormalization constants at  $O(\alpha)$ . They do not take into account one-loop mixing with  $1/M$  current operators or the discretization correction that arises at  $O(\alpha(a\Lambda_{QCD}))$ . We expect that at comparable  $\beta$  and  $M$  these two corrections should be of similar size in their formalism as we find here ( $\sim 3 - 5\%$ ). In spite of the range of approaches and approximations used, it is, nevertheless, encouraging to see that very different formulations of heavy quarks give results for  $f_B$  and  $f_{B_s}$  that are consistent within errors. The ratio  $f_{B_s}/f_B$ , in which many of the errors cancel, shows a larger spread among the groups. The NRQCD number lies  $1 \sim 2\sigma$  higher than the more recent relativistic heavy quark results in Table 6 by APE, Fermilab and MILC.

Our  $B$  meson decay constant results are still within the quenched approximation and at a fixed value of the lattice spacing. Calculations are underway to address these sources of uncertainty. The first results from  $n_f = 2$  dynamical configurations (without the  $1/M^2$  tree-level corrections) show that, within current statistical and systematic errors, unquenching effects are not yet visible [22]. Higher statistics and smaller dynamical quark masses are required to resolve this issue. Since we are using improved actions and currents we expect scaling violations to be small in quenched calculations at  $\beta = 6.0$ . Further quenched simulations at other

Collaboration	$f_B$ [MeV]	$f_{B_s}$ [MeV]	$f_{B_s}/f_B$
This work	$147^{(+17)}_{(-20)}$	$175^{(+18)}_{(-18)}$	$1.20^{(+6)}_{(-4)}$
APE [8]	180(32)	205(35)	1.14(8)
Fermilab [9]	$164^{(+16)}_{(-14)}$	$185^{(+16)}_{(-11)}$	$1.13^{(+5)}_{(-4)}$
JLQCD [10]	163(16)	175(18)	
MILC [11]	$153^{(+40)}_{(-16)}$	$164^{(+50)}_{(-16)}$	1.10(6)
UKQCD [12]	$160^{(+53)}_{(-20)}$	$194^{(+62)}_{(-10)}$	1.22(4)

Table 6: Comparison with quenched results for  $f_B$ ,  $f_{B_s}$  and  $f_{B_s}/f_B$  from recent lattice calculations using relativistic quarks. Errors include statistical and systematic errors, added in quadrature.

lattice spacings ( $\beta = 5.7$  and  $\beta = 6.2$ ) have been initiated to check this. Preliminary results at  $\beta = 5.7$  on UKQCD configurations are encouraging [23], however, to make any definitive statement requires a full analysis at all three  $\beta$  values.

## 5 Summary

This article describes a quenched calculation of  $B$  meson decay constants,  $f_B$  and  $f_{B_s}$ , using NRQCD  $b$ -quarks and clover light quarks. Tree-level corrections to the heavy quark action and the heavy-light currents have been included through  $O(1/M^2)$ . The full  $O(\alpha/M)$  matching between continuum QCD and lattice NRQCD currents has been incorporated together with an  $O(a\alpha)$  discretization correction to the heavy-light axial current. This is the first time both mass-dependent matching factors and the  $O(a\alpha)$  current correction have been included in a lattice determination of  $f_B$ . Our final results for  $f_B$ ,  $f_{B_s}$  and  $f_{B_s}/f_B$  are given in eqs. (16) and (18). The next step in our program is to study unquenching, scaling and finite volume effects, in addition to improving statistics. Work is already in progress on these fronts.

### Acknowledgements

This work has been supported by grants from the US Department of Energy, (DE-FG02-91ER40690, DE-FG03-90ER40546, DE-FG05-84ER40154, DE-FC02-91ER75661, DE-LANL-ERWE161), NATO (CRG 941259), PPARC and the Royal Society of Edinburgh. A. Ali Khan is grateful to the Graduate School of the Ohio State University for a University Postdoctoral Fellowship. C. Davies thanks the Institute for Theoretical Physics, Santa Barbara, for hospitality and the Leverhulme Trust and Fulbright Commission for funding while this work was being completed. J. Sloan would like to thank the Center for Computational Sciences, University of Kentucky, for support. We thank Joachim Hein, Peter Lepage and Tetsuya Onogi for useful discussions. The simulations reported here were done on CM5's at the Advanced Computing Laboratory at Los Alamos under a DOE Grand Challenges award, and at NCSA under a Metacenter allocation.

## References

- [1] For recent reviews see :  
J. Flynn, Nucl. Phys. **B** (Proc. Suppl.) **53**, 168 (1997);  
T. Onogi, Nucl. Phys. **B** (Proc. Suppl.) **63**, 59 (1998);  
A. Ali Khan, Nucl. Phys. **B** (Proc. Suppl.) **63**, 71 (1998).
- [2] G. P. Lepage *et al.*, Phys. Rev. D **46**, 4052 (1992).
- [3] B. Sheikholeslami and R. Wohlert, Nucl. Phys. **B259**, 572 (1985).
- [4] J. Shigemitsu, Nucl. Phys. **B** (Proc. Suppl.) **60A**, 134 (1998);  
C. Morningstar and J. Shigemitsu, Nucl. Phys. **B** (Proc. Suppl.) **63**, 341 (1998);  
C. Morningstar and J. Shigemitsu, hep-lat/9712016.
- [5] S. Collins *et al.*, Phys. Rev. D **55**, 1630 (1997);  
A. Ali Khan *et al.*, Phys. Rev. D **56**, 7012 (1997);  
S. Collins *et al.*, Nucl. Phys. **B** (Proc. Suppl.) **53**, 389 (1997).
- [6] A. Ali Khan *et al.*, Nucl. Phys. **B** (Proc. Suppl.) **53**, 368 (1997).
- [7] K. Ishikawa *et al.*, Phys. Rev. D **56**, 7028 (1997);  
K. Ishikawa *et al.*, Nucl. Phys. **B** (Proc. Suppl.) **63**, 344 (1998);  
N. Yamada *et al.*, Nucl. Phys. **B** (Proc. Suppl.) **63**, 350 (1998).
- [8] C. R. Allton *et al.*, Phys. Lett. **B405**, 133 (1997).
- [9] Fermilab Collaboration, A. El-Khadra *et al.*, hep-ph/9711426.
- [10] JLQCD Collaboration, S. Aoki *et al.*, hep-lat/9711041.
- [11] MILC Collaboration, C. Bernard *et al.*, Nucl. Phys. **B** (Proc. Suppl.) **63**, 362 (1998).
- [12] UKQCD Collaboration, R. M. Baxter *et al.*, Phys. Rev. D **49**, 1594 (1994).
- [13] A. El-Khadra, A. Kronfeld and P. Mackenzie, Phys. Rev. D **55**, 3933 (1997).
- [14] G. P. Lepage and P. B. Mackenzie, Phys. Rev. D **48**, 2250 (1993).
- [15] N. Isgur, proceedings of the Uehling Summer School on Phenomenology and Lattice QCD, Seattle, WA, 21 June – 2 July 1993, ed. by G. Kilcup and S. Sharpe, World Scientific, p. 63 (1995).
- [16] A. Ali Khan *et al.*, in preparation.
- [17] DELPHI Collaboration, DELPHI 96-93 CONF 22, contribution to ICHEP '96.
- [18] DELPHI Collaboration, DELPHI Note 95-107, contribution to EPS'95.
- [19] K. Jansen *et al.*, Phys. Lett. **B372**, 275 (1996).

- [20] O. Hernandez and B. Hill, Phys. Rev. D **50**, 495 (1994).
- [21] J. Hein *et al.*, work in progress.
- [22] S. Collins *et al.*, in preparation. See also the third article in [1].
- [23] J. Hein *et al.*, Nucl. Phys. **B** (Proc. Suppl.) **63**, 347 (1998).